



## Development of a 22 GHz ground-based spectrometer for middle atmospheric water vapour monitoring

Pietro Paolo Bertagnolio, Giovanni Muscari & James Baskaradas

To cite this article: Pietro Paolo Bertagnolio, Giovanni Muscari & James Baskaradas (2012) Development of a 22 GHz ground-based spectrometer for middle atmospheric water vapour monitoring, European Journal of Remote Sensing, 45:1, 51-61, DOI: [10.5721/EuJRS20124506](https://doi.org/10.5721/EuJRS20124506)

To link to this article: <https://doi.org/10.5721/EuJRS20124506>



© 2012 The Author(s). Published by Taylor & Francis.



Published online: 17 Feb 2017.



Submit your article to this journal [↗](#)



Article views: 44



View related articles [↗](#)

---

# Development of a 22 GHz ground-based spectrometer for middle atmospheric water vapour monitoring

Pietro Paolo Bertagnolio<sup>1,2\*</sup>, Giovanni Muscari<sup>1</sup> and James Baskaradas<sup>1</sup>

<sup>1</sup>Istituto Nazionale di Geofisica e Vulcanologia, via di Vigna Murata, 605 - 00143 Roma

<sup>2</sup>Dipartimento di Scienze della Terra, Università di Siena, via del Laterino, 8 - 53100 Siena

\*Corresponding author, e-mail address: pietropaolo.bertagnolio@ingv.it

## Abstract

The water Vapour Emission SPectrometer for Antarctica at 22 GHz (VESPA-22) has been designed for long-term middle atmospheric climate change monitoring and satellite data validation. It observes the water vapour spectral line at 22.235 GHz using the balanced beam-switching technique. The receiver antenna has been characterized, showing an HPBW of 3.5° and a sidelobe level 40 dB below the main lobe. The receiver front-end has a total gain of 105 dB and a LNA noise temperature of 125 K. A FFT spectrometer (bandwidth 1 GHz, resolution 63 kHz) will be used as back-end, allowing the retrieval of H<sub>2</sub>O concentration profiles in the 20 to 80 km altitude range. The control I/O interface is based on reconfigurable hardware (USB-CPLD).

**Keywords:** Microwave remote sensing, water vapour, stratosphere, Antarctica, antenna measurements.

## Introduction

Water vapour is a crucial element of the climate system. Accurate observations of stratospheric humidity are needed in the equatorial belt, where water vapour crosses the tropopause, and in the polar regions, that are affected the most by climate change trends [IPCC, 2007; Solomon et al., 2010]. Satellite-based observations provide atmospheric composition data with extensive spatial and temporal coverage, but these need to be validated and integrated by ground-based networks like GAW (Global Atmospheric Watch) and NDACC (Network for Detection of Atmospheric Composition Change). Moreover, it was shown that changes in middle atmospheric water vapour on time scales longer than the duration of a satellite mission can be successfully observed by ground-based instruments [Nedoluha et al., 2009]. Several other ground-based spectrometers have been developed in the last decades to detect the water vapour rotational emission line at 22.235 GHz with heterodyne microwave receivers [e.g., Nedoluha et al., 2009; Straub et al., 2011]. Due to the collisional (or pressure) broadening of spectral lines in the microwave region, the vertical distribution of water vapour can be retrieved from the measured spectra using inverse techniques, such as the Optimal Estimation Method (OEM) [Rodgers, 2000].

A new ground-based spectrometer for the observation of middle atmospheric water vapour concentration profiles has been designed at the Istituto Nazionale di Geofisica

e Vulcanologia (INGV) in Rome (Fig. 1), and a first set of tests is presented here. The water Vapour Emission SPectrometer for Antarctica at 22 GHz (VESPA-22) has two main science objectives: provide long-term (decadal time scale) as well as short-term (diurnal) observations of water vapour variations from observatories at high altitude/high latitude (characterized by low atmospheric opacity). In order to observe diurnal changes in the mesosphere, we aim at obtaining spectra (at the full resolution  $B$  of 61 kHz) with a signal-to-noise ratio (SNR) of 115 with a total integration time ( $t_{tot}$ ) of 12 hours (Table 1). Faster changes in the lower stratosphere can be observed with a  $t_{tot}$  of 1 hour (and the same SNR) by reducing the spectral resolution to 610 kHz.

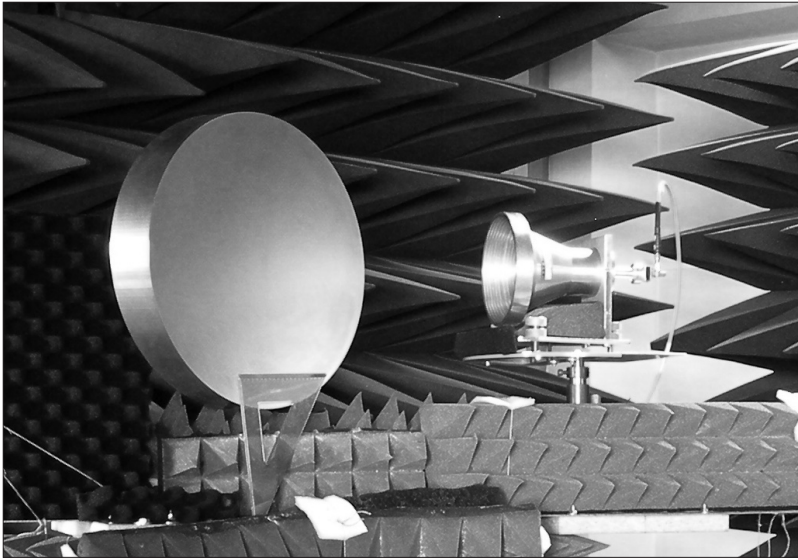


**Figure 1 - The VESPA-22 parabolic off-axis reflector and feed horn antenna under test in the indoor test site at ISCTI, Rome.**

This will be achieved by having a system temperature ( $T_{sys}$ ) of  $\approx 165$  K and an effective observation time  $t$  of 4.8 hours, that is a percentage of operating time dedicated to observing the atmospheric signal of 40%. It is shown that system temperatures in this range can be obtained using an uncooled low-noise-amplifier at 22 GHz of the latest generation [e.g., Forkman et al., 2002; Deuber et al., 2004]. The need to maximise the effective observation time led us to adopt a balanced beam-switching configuration with a chopper mirror rotating at  $\sim 1$  Hz [e.g., Parrish et al., 1988; de Zafra and Muscari, 2004, and references therein]. Balanced beam-switching receivers use the sky near the zenith direction as a calibration reference, with a weak grey-body emission added in the “reference” beam so to have the same wide-band power as the “signal” beam (usually pointing 10-20° above the horizon). The difference spectrum (signal – reference / reference) is then not affected by channel-dependent gain variations, which would compromise the detection of weak emission lines. The VESPA-22 specification parameters have been calculated using the radiometer noise formula for a balancing radiometer [modified from Janssen, 1993]:

$$\sigma = c_{trop} \frac{2T_{sys}}{\sqrt{Bt}} \quad [1]$$

where  $\sigma$  is the goal noise level in kelvin. The tropospheric correction coefficient  $c_{trop}$  is used to scale the spectrum from the “signal” beam angle to the zenith direction, and it depends on the observation angle itself (assumed between 10° and 15° above the horizon) and the tropospheric opacity (assumed between 0.007 and 0.06, consistent with a high altitude/high latitude site [e.g., Deuber et al., 2005; Straub et al., 2011]). The goal specification for absolute accuracy of the retrieved mixing ratio profile is 15%, with the specified SNR, based on previous experience with the OEM.

**Table 1 - Observation goals and instrument specifications.**

Observation goals		Instrument specifications	
Observation angle	10°-15°	Spectral resolution ( $B$ )	61 kHz
Signal-to-noise ratio (SNR)	115	Spectrometer bandwidth	1 GHz
Total integration time ( $t_{tot}$ )	12 hrs (1 h if binned)	Antenna beamwidth (HPBW)	3.5°
Altitude range of profiles	20 - 80 km	Effective observation time ( $t / t_{tot}$ )	40%
Profile accuracy	15%	System temperature ( $T_{sys}$ )	≈ 165 K

The long-term accuracy of measured spectra is guaranteed by constant calibration against three different references: i) the “reference” beam, measured every chopper cycle, ii) calibrated noise diodes, whose output is added to the measured atmospheric signal for a cycle every ~20 minutes, iii) hot and cold loads at controlled temperatures for an absolute calibration on a monthly basis. Details on the calibration are reported in a later section. Additionally, the strategy for cross-calibrating the VESPA-22 long-term data set involves a first validation campaign with existing satellite water vapour measurements (e.g., Aura/MLS, ACE-FTS) at the end of the development and installation phases, and subsequent intercomparison campaigns before and after every major repair or upgrade of the equipment.

The proposed site for the installation of VESPA-22 is Concordia Station (3233 m asl, 75.1°S, 123.3°E, NDACC site), Antarctica. Alternative sites are Mount Chacaltaya, Bolivia (5320 m asl, 16.2°S, 68.1°W, GAW site), or Thule Air Base, Greenland (225 m asl, 76.5°N 68.8°W, NDACC site), where the Ground-Based Microwave Spectrometer (GBMS) [e.g., de Zafra and Muscari, 2004] is currently operated and performing regular measurements of stratospheric profiles of several trace gases.

### Description of the instrument

The radiation emitted by water vapour molecules in the atmosphere is collected, through an off-axis parabolic reflector and a feedhorn antenna, by a single side-band uncooled heterodyne receiver. Once the signal is properly amplified and down converted in frequency

(Fig. 2), a high resolution FFT spectrometer is used for digital acquisition. Both signal acquisition and control of the observation and calibration cycles are realized with a real-time PC-based system developed and tested at our laboratory.

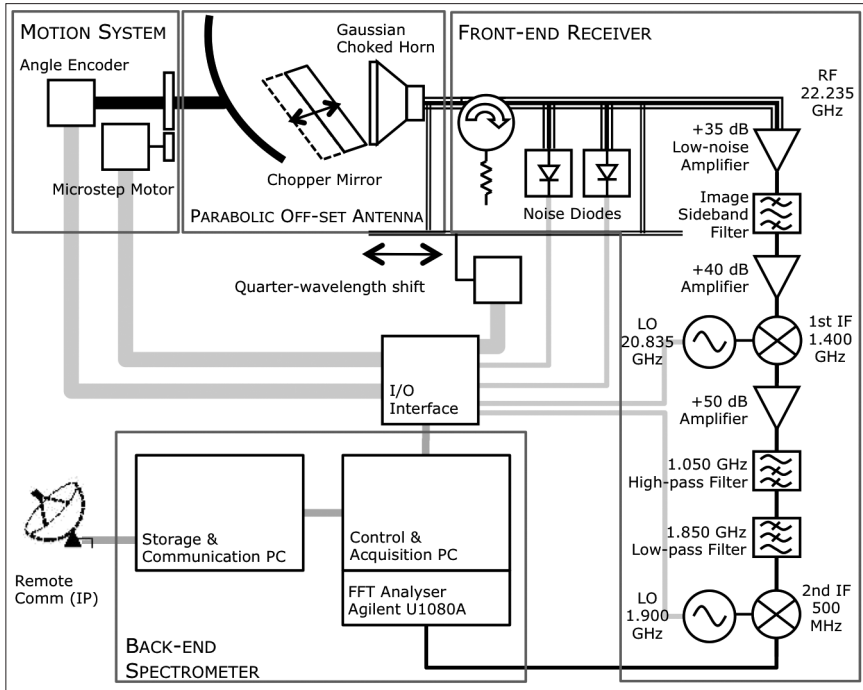


Figure 2 - Functional scheme of the VESPA-22 instrument.

### Receiver antenna

The antenna of VESPA-22 is composed by an off-axis parabolic reflector coupled with a feedhorn, providing a high directivity and a relatively compact instrument size.

The feedhorn for the antenna is an aluminium choked Gaussian horn designed and manufactured by the Public University of Navarra [Teniente et al., 2002]. The circular shape was chosen to have a consistent response from different observation angles, such as those necessary for the balanced beam-switching technique. The horn was designed to have a high Gaussian beam purity (99.85%) and low sidelobes in a 1.3 GHz band around 22.235 GHz.

The feedhorn was tested in operational conditions on the Water Vapour Microwave Spectrometer (WVMS2) [e.g., Nedoluha et al., 1995] at Table Mountain, California, to make sure that internal reflections did not produce any spectrally-dependent anomalies in the received signal (spectral artefacts). The test did not show any remarkable spectral artefact attributable to the feedhorn in a frequency range of 500 MHz around the  $\text{H}_2\text{O}$  line at 22.235 GHz. Figure 3 shows the measured signal intensity spectrum in brightness temperature units, as the radiation emitted at these frequencies is proportional to the emission temperature according to Rayleigh-Jeans' law. Relative temperature values are

indicated on the y-axis, as the signal emitted by tropospheric water vapour consists of a temperature offset in the pass band which is removed in the calibration process.

The beam-switching technique requires observations of the sky at different elevation angles with the same radiation response, thus a rotating reflector of some kind is needed. We chose to employ a parabolic off-axis reflector that can rotate around its optical axis (Fig. 1). The reflector was designed using the General Reflector Antenna Software Package (GRASP), considering size and directivity, and results in an overall antenna HPBW of  $3.5^\circ$ . Manufactured by Thomas Keating Ltd., it has an elliptical shape, with an aperture 40 cm wide, and a focal distance of 21 cm. The optimal distance between the reflector and the phase centre of the feedhorn was estimated at 43 cm using GRASP, where particular attention was devoted to minimize beam asymmetry and keep a low level of spill-over loss (now at 0.0019 dB).

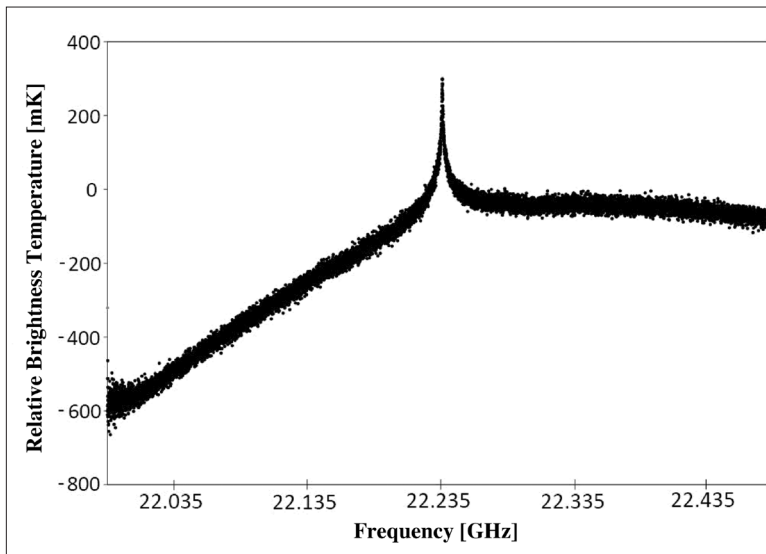


Figure 3 - The 22 GHz water vapour line observed by the WVMS2 instrument at Table Mountain, California, using the VESPA-22 feed horn. (Courtesy of G. Nedoluha and M. Gomez).

### *Front-end receiver*

The receiver employs the heterodyne principle to down-convert the observed signals centred around the 22.235 GHz water vapour line first to a 1.4 GHz intermediate frequency (IF), then to a 500 MHz second IF. The first IF was chosen for compatibility with back-end spectrometers (AOS and filterbanks) already in use at INGV. The second IF is optimised for the FFT back-end.

The first-stage amplifier is a very-low-noise miniature waveguide amplifier (LNA) from Miteq. Inc. with a noise temperature of 125 K and a +36 dB gain. An additional RF amplifier and a first IF amplifier provide a total gain of 105.6 dB for the whole chain. A double sideband mixer is employed, together with an image rejection filter with a pass

band between 21.5 and 23 GHz. The local oscillator signal at 20.835 GHz is provided by a tunable synthesizer with a high stability (better than 30 kHz).

### ***Digital motion control system***

The reflector elevation angle needs to be set and known to a high degree of accuracy, to make sure that the optical path uncertainty is small, and to provide proper balancing of the “signal” atmospheric and “reference” spectra. A high precision motion control system was designed to meet these needs. The rotating and holding torque is provided by a 51200-micrstep motor by Schneider Electric, linked to the main reflector axle by high precision aluminium gears with a ratio of 1:5. The angle of the reflector axle is tracked by a 13-bit absolute encoder by Lika Electronics, resulting in an overall precision on the elevation angle of 0.07°.

In order to minimize standing waves produced by internal reflections, the VESPA-22 design includes the opportunity for feedhorn and front-end receiver to be moved continuously back and forth by a quarter-wavelength distance with respect to the parabolic reflector by means of a micrstep linear actuator.

### ***Calibration procedure***

Periodical calibration is needed to account for time- and spectral-dependent variations in the receiver noise temperature. VESPA-22 is designed for a calibration procedure that is a modified version of the one described in Nedoluha et al. [1995]: a calibrated noise source injects a known power in the waveguide link between the feedhorn and the LNA via a 20-dB directional coupler, so that the intensity of the atmospheric signal can be assessed by acquiring the received signal with and without the calibrated noise power added. Two calibrated noise diodes with a 15-dB ENR by Noisecom will be used, with one as backup and reference for the other.

An absolute calibration will be performed on a monthly basis with a hot-cold scheme, using Eccosorb CV-3 **microwave absorbers in the observation beam, with the hot load at room temperature**, and the cold load immersed in liquid nitrogen at 77 K.

The motion system, the front-end receiver and the noise calibration system are connected to the control PC via a multi-purpose control-and-acquisition board developed at INGV. The digital I/O and control interface is based on a high speed USB peripheral controller (FX2LP) and a reconfigurable CPLD (XC95288XL), supporting up to 117 digital I/O lines. This combination forms a powerful, flexible and easy to use high speed interface.

### ***Back-end FFT spectrometer***

The microwave signals are acquired using an Agilent U1080A analyser board, with a fast Fourier transform (FFT) firmware running on the Virtex field-programmable gate array (FPGA) core. The ADC converter acquires at a frequency of 2 gigasamples per second, resulting (by Nyquist sampling theorem) in a spectral range of 0 to 1 GHz. Since the firmware computes FFT spectra on 16384 channels, a spectral resolution of 61 kHz is achieved [Benz et al., 2005]. The bandwidth and the resolution lead to an observation range between 20 km and 80 km altitude, based on the estimates by Janssen [1993] for the 22 GHz water vapour line. The FFT spectrometer board is mounted on a cPCI chassis and controlled through a PCI-cPCI bus by the control PC, running a custom acquisition software written in LabView and running under the LabView Real-Time OS.

## Characterization of the antenna system

The performance of the receiver antenna system was measured in the lab, to make sure that design specifications would be met, and to test the reliability of the motion system. The Microwave Eurolab laboratories of the Istituto Superiore delle Comunicazioni e delle Tecnologie dell'Informazione (ISCTI) in Rome provided with testing equipment and facilities. The far-field spectral-dependent antenna pattern was measured for both the feedhorn and the complete antenna system. Moreover, near-field phase measurements were performed on the feedhorn alone. The boresight antenna gain was measured in both indoor and outdoor test ranges using the gain-transfer method described by Rudge [1982]. In this method a gain-standard antenna is used as reference, and its measured signal power is compared to the power measured with the antenna under test. The measured power difference is then equal to the gain difference.

### *Far-field feedhorn measurements*

The far-field characterization of the feed horn alone was achieved in a semi-anechoic chamber, certified by ETSI as an "indoor site" for tests on radio- and microwave-frequency telecommunications devices. A calibrated horn antenna (by Flann Microwave Ltd.) with a gain of 20.0 dBi ( $\pm 0.1$  dBi) at 22.2 GHz was used as source antenna. It was set on a tripod at a  $\sim 4$  m distance from the feed horn, mounted on an azimuth-rotating support. A signal generator Anritsu 69367B was used to produce a sine wave signal sweeping a 2 GHz range centred at 22.235 GHz with a resolution of 5 MHz. The signal received by the feed horn was amplified by a HP 83051A pre-amplifier and measured with a scalar signal analyser R&S FSQ40. Azimuth scans were performed rotating the feed horn on the horizontal plane with a variable angle step ( $0.5^\circ$  to  $3^\circ$ ). Both principal planes (E-plane and H-plane) were scanned, in both co-polar and cross-polar configurations.

From the antenna pattern observed at 22.235 GHz in both principal planes (not shown), the half-power beam-width (HPBW) of the feed horn alone is measured at approximately  $12.5^\circ$ , and the first-null beam-width (FNBW) is approximately  $60^\circ$ . The first side lobe has an intensity more than 35 dB lower than that of the main lobe. The maximum intensity measured in cross-polar configuration is also 35 dB lower than the co-polar main lobe peak. Along the whole spectral range observed the only significant spectral-dependent feature in the antenna pattern is a widening of the main lobe with decreasing frequency, as expected. A gain-transfer test was performed using an additional Flann calibrated horn antenna as reference, resulting in a gain of 21.8 dBi ( $\pm 0.2$  dBi) for the feed horn of VESPA-22.

### *Near-field feed horn measurements*

In order to check whether the reflector and the feed horn were properly matched, the microwave beam entering the feed horn was characterised with a near-field scan at the distance between the reflector surface and the feed horn phase centre. The measurement setup had a Wiltron 360 B vector network analyser with a coax-waveguide (WR-42) transition as source antenna and the feed horn as receiving antenna, placed on an azimuth-rotating structure and connected to an HP 83051A pre-amplifier. By rotating the feed horn around its Gaussian beam phase centre on both principal planes and measuring the phase variation, we verified that the curvature of the wave front of the beam matched the curvature of the spherical reflector. We could observe a phase deviation of less than 0.1 radians in a  $10^\circ$  interval from the boresight direction (Fig. 4).



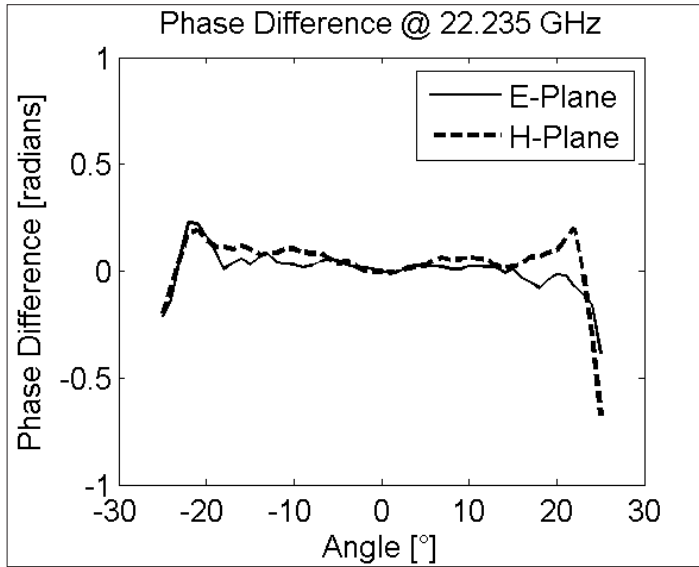


Figure 4 - Phase difference from the boresight direction for the VESPA-22 feed horn alone at a 43 cm distance.

#### *Far-field antenna system measurements*

The far-field of the complete antenna system (parabolic reflector and feed horn) was characterised using the same setup as the far-field azimuth scans on the feed horn, with the antenna motion system used to set the elevation angle. The complete spectral-dependent antenna pattern was therefore measured indoors at a 4 m distance (Fig. 5).

However, since the whole antenna has a Fraunhofer distance of 24 m, larger than the size of the anechoic chamber, we repeated outdoors, at a 34.5 m distance, the measurements at 22.235 GHz. For the outdoor measurements the rooftop of a L-shaped building >20 m high was chosen as test site, with the source and the receiver antennas placed on the two segments of the L-shape so that the beam would travel more than 20 m above the ground, with no metal structures in the field of view of the antennas. This configuration was judged a good approximation of a free-space elevated range by the absence of reflected signals at different angles. No significant difference was observed between the indoor and outdoor data sets. Both principal planes were scanned in both co-polar and cross-polar configurations for the two main observation geometries of the antenna, “signal” and “reference”.

The HPBW  $\Theta_{3\text{dB}}$  (averaged over the 4 configurations) is  $3.5^\circ (\pm 0.1^\circ)$ , resulting in a directivity ( $D_M 4\pi / \Theta_{3\text{dB E}} \Theta_{3\text{dB H}}$ ) of 35 dBi ( $\pm 2$  dBi), while the FNBW is approximately  $30^\circ$ . The side lobe level is more than 40 dB below the boresight gain, as expected from the GRASP simulations. Cross-polarization rejection is now lower than it was with the feedhorn alone, as can be seen by the difference between the maximum received power in co-polar and cross-polar configuration being lower than before (24 dB versus the 35 dB of the feed horn alone). In Figure 6, the “signal” configuration pattern at 22.235 GHz, both expected (right panel) and measured (left panel), is presented (the “reference” configuration does not show any significant difference). Due to the larger directivity of the whole antenna

system with respect to the feedhorn alone, the beamwidth variation with frequency is less significant (Fig. 5). An antenna gain of 33.3 dBi ( $\pm 0.2$  dBi) was measured using the gain-transfer method.

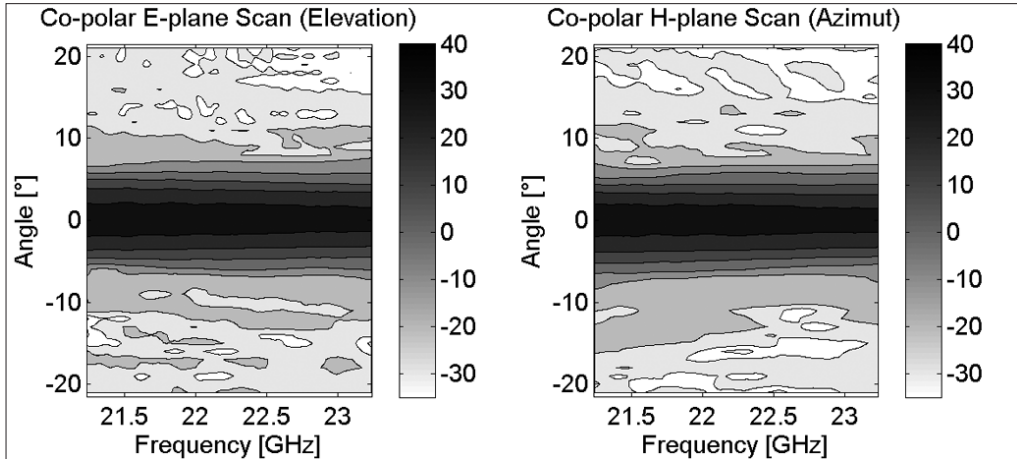


Figure 5 - Spectral-dependent antenna pattern of the VESPA-22 antenna system measured in the indoor site at ISCTI in co-polar “signal” configuration. On the left, elevation scan of the E-plane; on the right, azimuth scan of the H-plane.

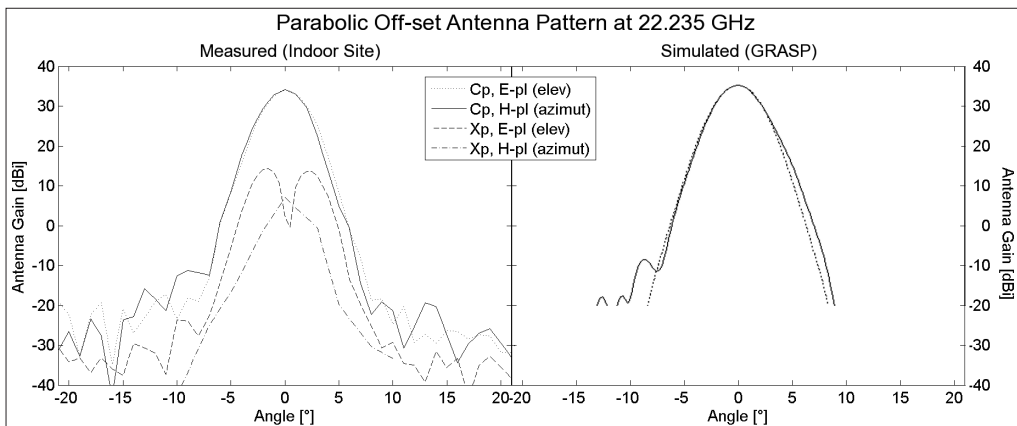


Figure 6 - Antenna pattern of the VESPA-22 antenna (off-axis parabolic reflector and corrugated feed horn) at 22.235 GHz simulated using GRASP (right) and measured in the “indoor site” at ISCTI (left).

## Conclusions and future work

The VESPA-22 has been designed as a middle atmospheric water vapour monitoring station, to retrieve concentration profiles from about 20 to 80 km altitude and observe their long-term (decadal) and short-term (diurnal) changes. The receiver antenna has been

characterised, and it showed a HPBW of  $3.5^\circ$  and sidelobe levels more than 40 dB below the main lobe, with no significant spectral dependence.

Further steps in the development include: in February 2011, a test of the back-end FFT spectrometer on the GBMS spectrometer at Thule Air Base and comparison with the existing AOS system and, in autumn 2011, the final assembling and test of the front-end receiver, with a measurement of the actual receiver noise temperature. The first atmospheric observations are planned for spring 2012.

## Acknowledgements

We gratefully acknowledge the valuable cooperation and support from:

R. de Zafra, State University of New York at Stony Brook; M. Gomez and G. Nedoluha, Naval Research Laboratory, Washington DC, USA; A. Murk, Institut für Angewandte Physik, Universität Bern, Switzerland; E. Restuccia, R. Dal Molin and G. Pierri, Istituto Superiore per le Comunicazioni e delle Tecnologie dell'Informazione, Rome, Italy.

## References

- Benz A. O., Grigis P. C., Hungerbühler V., Meyer H., Monstein C., Stuber B., Zardet D. (2005) - *A broadband FFT spectrometer for radio and millimeter astronomy*. *Astronomy & Astrophysics*, 442: 767-773. doi: <http://dx.doi.org/10.1051/0004-6361:20053568>.
- Deuber B., Kämpfer N., Feist D. G. (2004) - *A New 22-GHz Radiometer for Middle Atmospheric Water Vapor Profile Measurements*, *IEEE T. Geosci. Remote*, 42, 974–984. 3362. doi: <http://dx.doi.org/10.1109/TGRS.2004.825581>.
- Deuber B., Morland J., Martin L., Kämpfer N. (2005) - *Deriving the tropospheric integrated water vapor from tipping curve-derived opacity near 22 GHz*. *Radio Science*, 40(5), 1-11. doi:10.1029/2004RS003233
- de Zafra R. L., Muscari G. (2004) - *CO as an important high-altitude tracer of dynamics in the polar stratosphere and mesosphere*. *J. Geophys. Res.* 109: D06105. doi: <http://dx.doi.org/10.1029/2003JD004099>.
- Forkman P., Eriksson P., Winnberg A. (2002) - *The 22 GHz radio-aeronomy receiver at Onsala Space Observatory*, *J. Quant. Spec. Rad. Trans.*, Vol 77, 1, pag.23-42. doi: [http://dx.doi.org/10.1016/S0022-4073\(02\)00073-0](http://dx.doi.org/10.1016/S0022-4073(02)00073-0).
- IPCC (2007) - *Climate Change 2007: The Physical Science Basis. Contribution of Working Group I to the Fourth Assessment Report of the Intergovernmental Panel on Climate Change*. Cambridge University Press, Cambridge, United Kingdom and New York, NY, USA.
- Janssen M. A. (1993) - *Atmospheric remote sensing by microwave radiometry*. John Wiley, New York. p. 24.
- Nedoluha G. E., Bevilacqua R. M., Gomez R. M., Thacker D. L., Waltman W. B., Pauls T. A. (1995) - *Ground-based measurements of water vapor in the middle atmosphere*, *J. Geophys. Res.*, 100(D2), 2927–2939, doi: <http://dx.doi.org/10.1029/94JD02952>.
- Nedoluha G. E., Gomez R. M., Hicks B. C., Wrotny J. E., Boone C., Lambert A. (2009) - *Water vapor measurements in the mesosphere from Mauna Loa over solar cycle 23*, *J. Geophys. Res.*, 114, D23303. doi: <http://dx.doi.org/10.1029/2009JD012504>.
- Parrish A., deZafra R. L., Solomon P. M., Barrett J. W. (1988) - *A ground-based technique*

- for millimeter wave spectroscopic observations of stratospheric trace constituents.* Radio Science. 23(2): 106–118. doi: <http://dx.doi.org/10.1029/RS023i002p00106>.
- Rodgers C. D. (2000) - *Inverse method for atmospheric sounding: theory and practice.* World Scientific Publishing Co., Singapore.
- Rudge A. W. (1982) - *The handbook of antenna design: 1.* Peregrinus, London. pp. 650-651. doi: <http://dx.doi.org/10.1049/PBEW015F>.
- Solomon S., Rosenlof K. H., Portmann R. W., Daniel J. S., Davis S. M., Sanford T. J., Plattner G. K. (2010) - *Contributions of Stratospheric Water Vapor to Decadal Changes in the Rate of Global Warming.* Science, 327: 1219-1223. doi: <http://dx.doi.org/10.1126/science.1182488>.
- Straub C., Murk A., Kämpfer N., Golchert S. H., Hochschild G., Hallgren K., Hartogh P. (2011) - *ARIS-Campaign: intercomparison of three ground based 22 GHz radiometers for middle atmospheric water vapor at the Zugspitze in winter 2009.* Atmos. Meas. Tech., 4(9), 1979-1994, doi:10.5194/amt-4-1979-2011.
- Teniente R., Goni D., Gonzalo R., del-Rio C. (2005) - *Choked Gaussian Antenna: extremely low sidelobe compact antenna design.* IEEE Antennas and Wireless Propagation Letters, 1: 200 – 202. doi: <http://dx.doi.org/10.1109/LAWP.2002.807959>.

**Received 17/02/2011, accepted 21/07/2011**

© 2012 by the authors; licensee Italian Society of Remote Sensing (AIT). This article is an open access article distributed under the terms and conditions of the Creative Commons Attribution license (<http://creativecommons.org/licenses/by/4.0/>).